

# Naval Research Laboratory

Washington, DC 20375-5320



NRL/MR/6750--03-8718

## Ion and Electron Currents to Electrodes in Pulsed Electron Beam-Produced Plasmas

DARRIN LEONHARDT

SCOTT WALTON

RICHARD FERNSLER

ROBERT A. MEGER

*Charged Particle Physics Branch*

*Plasma Physics Division*

CHRIS MURATORE

*ASEE-NRL Postdoctoral Research Associate*

DAVID BLACKWELL

*SFA, Inc.*

*Largo, MD*

November 7, 2003

20031201 130

Approved for public release; distribution is unlimited.

# REPORT DOCUMENTATION PAGE

Form Approved  
OMB No. 0704-0188

Public reporting burden for this collection of information is estimated to average 1 hour per response, including the time for reviewing instructions, searching existing data sources, gathering and maintaining the data needed, and completing and reviewing this collection of information. Send comments regarding this burden estimate or any other aspect of this collection of information, including suggestions for reducing this burden to Department of Defense, Washington Headquarters Services, Directorate for Information Operations and Reports (0704-0188), 1215 Jefferson Davis Highway, Suite 1204, Arlington, VA 22202-4302. Respondents should be aware that notwithstanding any other provision of law, no person shall be subject to any penalty for failing to comply with a collection of information if it does not display a currently valid OMB control number. PLEASE DO NOT RETURN YOUR FORM TO THE ABOVE ADDRESS.

1. REPORT DATE (DD-MM-YYYY) November 7, 2003		2. REPORT TYPE Interim Report		3. DATES COVERED (From - To)	
4. TITLE AND SUBTITLE  Ion and Electron Currents to Electrodes in Pulsed Electron Beam-Produced Plasmas				5a. CONTRACT NUMBER	
				5b. GRANT NUMBER 67-7641-04	
				5c. PROGRAM ELEMENT NUMBER	
6. AUTHOR(S)  Darrin Leonhardt, Scott Walton, Chris Muratore, * David Blackwell,† Richard Farnsler, and Robert A. Meger				5d. PROJECT NUMBER	
				5e. TASK NUMBER	
				5f. WORK UNIT NUMBER	
7. PERFORMING ORGANIZATION NAME(S) AND ADDRESS(ES)  Naval Research Laboratory, Code 6750 4555 Overlook Avenue, SW Washington, DC 20375-5320				8. PERFORMING ORGANIZATION REPORT NUMBER  NRL/MR/6750--03-8718	
9. SPONSORING / MONITORING AGENCY NAME(S) AND ADDRESS(ES)  Office of Naval Research 800 North Quincy Street Arlington, VA 22217				10. SPONSOR / MONITOR'S ACRONYM(S)	
				11. SPONSOR / MONITOR'S REPORT NUMBER(S)	
12. DISTRIBUTION / AVAILABILITY STATEMENT  Approved for public release; distribution is unlimited.					
13. SUPPLEMENTARY NOTES  *ASEE-NRL Postdoctoral Research Associate †SFA, Inc., Largo, MD					
14. ABSTRACT  Electron and ion currents to various electrodes in pulsed, electron beam-produced plasmas were measured in a number of laboratory systems. These experiments showed variations in the measured currents that depended on gas type, cathode material, magnetic field geometry, and electrode impedance. Explanations of these observations are given on a per case basis, after a careful evaluation and comparison of all other experimental factors.					
15. SUBJECT TERMS  LAPPS; Plasma processing; Hollow cathode					
16. SECURITY CLASSIFICATION OF:  a. REPORT Unclassified		17. LIMITATION OF ABSTRACT  b. ABSTRACT Unclassified		18. NUMBER OF PAGES  c. THIS PAGE Unclassified	19a. NAME OF RESPONSIBLE PERSON Darrin Leonhardt
				23	19b. TELEPHONE NUMBER (include area code) 202-767-7532

## CONTENTS

ABSTRACT .....	1
PREFACE .....	1
LARGE LAPPS CHAMBER .....	3
STAINLESS STEEL EQP CHAMBER .....	9
ALUMINUM PROCESSING CHAMBER .....	12
STAINLESS STEEL PROCESSING ('SPUTTERING') CHAMBER .....	16
SUMMARY AND CONCLUSIONS .....	17
ACKNOWLEDGMENTS .....	20
REFERENCES .....	20

## ION AND ELECTRON CURRENTS TO ELECTRODES IN PULSED ELECTRON BEAM-PRODUCED PLASMAS\*

*Darrin Leonhardt, Scott Walton, Chris Muratore<sup>†</sup>, David Blackwell<sup>‡</sup>,*

*Richard Fernsler and Robert Meger*

*Plasma Physics Division, Naval Research Laboratory, Washington, DC*

### Abstract

Electron and ion currents to various electrodes in pulsed, electron beam-produced plasmas were measured in a number of laboratory systems. These experiments showed variations in the measured currents that depended on gas type, cathode material, magnetic field geometry and electrode impedance. Explanations of these observations are given on a per case basis, after a careful evaluation and comparison of all other experimental factors.

### Preface

*The following data and discussion is focused on measurements taken in various plasma reactors. This information is intended for researchers familiar with the NRL LAPPS work and systems, thus a great deal of the general experimental detail has been omitted. This particular work is not intended to be a complete scientific work or tutorial on the LAPPS technology, but a comparison between active plasma systems in our laboratories.*

---

\* *This work supported by the Office of Naval Research*

<sup>†</sup> *ASEE/NRL Postdoctoral Research Associate*

<sup>‡</sup> *SFA Inc., Largo, MD*

In order to get baseline values for the electrode currents in the large LAPPs chamber, a series of measurements were made using a systematic set of operating conditions. This approach was taken to determine which effects were due to the measurement itself and which could be attributed to the actual operation of the e-beam produced plasma. These experiments were necessary because beam dump currents measured previously varied with the termination to ground (see Fig 1). This data implied that the beam dump was a more dynamic part in the system than previously considered, perhaps because the termination resistance was similar to the plasma resistance.

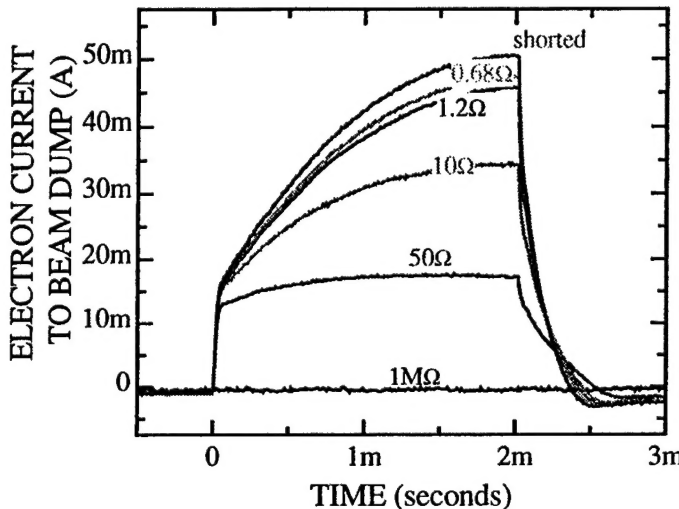
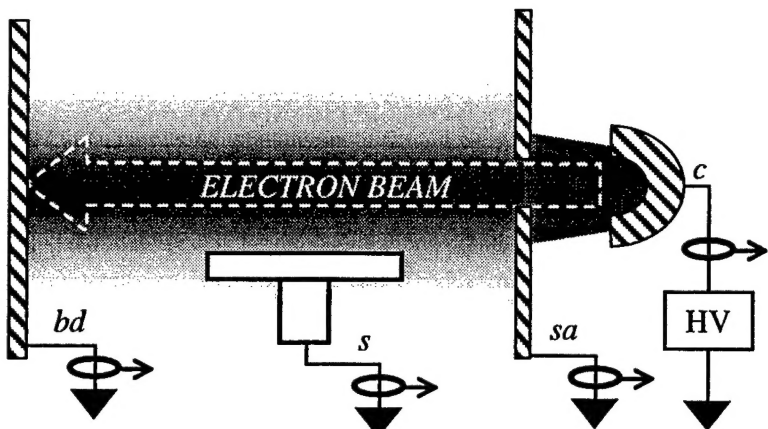


**FIGURE 1** Electron currents measured to beam dump electrode in large area chamber for a 2 ms plasma pulse. Electrode termination values accompany data.

The total current must always be conserved, so in an ideal system (without chamber walls)  $I_{\text{cath}} = I_{\text{stage}} + I_{\text{slot}} + I_{\text{dump}}$ . However, in real plasma processing systems there are many conducting surfaces available and it is nearly impossible to measure all current paths. Furthermore, not all current paths are as simple as initially believed, which will be illustrated by these experiments. In the present experiments, currents to the beam dump anode, slotted anode, and various stages were measured. All stages and the slotted anode were grounded while the beam dump anode was typically terminated into  $50\Omega$ . These values were chosen to have the beam dump anode at a higher impedance to draw little plasma current and allow the stages to act as the primary ground reference for the plasma. (It should be noted that all stages contained a ground shield that could also conduct plasma currents, but were not monitored.) Similar conditions were applied to the other pulsed cathode systems (stainless steel EQP chamber, stainless steel processing chamber and the aluminum processing chamber) for comparison. A general experimental layout is given in Fig 2, with variations between the experimental systems outlined the appropriate section. All currents were measured using identical Pearson Electronics Model 110 current transformers<sup>1</sup>.

**FIGURE 2** General schematic diagram showing hollow cathode (c), slotted anode (sa), beam dump anode (bd) and a processing stage (s). Circles with arrows represent current transformers. The cathode groove and anode slot are both 1 cm wide and of comparable lengths.



### LARGE LAPPS CHAMBER

An argon plasma (56 mT/150 Gauss field) was produced<sup>2</sup> by a linear hollow cathode run with a -2 kV, 2 ms pulse at 10% and 40% duty factors (DF). The cathode operating voltage, measured by the voltage divider during the pulse, was held constant in these and all subsequent measurements. The hollow cathode was made from stainless steel rod with a 1 cm wide by 1.5 cm deep groove running 50 cm of the 51 cm length. The beam dump anode was a 5 cm wide piece of copper tape long enough to intercept the entire beam located ~ 1 meter from the cathode and terminated outside the chamber (measured capacitance of 1.1 nF). The small (50 cm<sup>2</sup>) and large (64 cm x 90 cm) processing stages were in the chamber. The small stage (measured capacitance 25 pF) was grounded externally while the large stage was grounded inside the chamber. On top of the large stage was a smaller (600 cm<sup>2</sup>) isolated 'stage' made from copper tape (measured capacitance 1.7 nF), which was grounded outside the chamber. The slotted anode was fastened to the cathode support structure, and thereby grounded inside the chamber at the cathode. The magnetic field on this system was solenoidal. Gas flow was ~ 200 sccm. The cathode current was the electron current from the power supply to the cathode. All currents reported here are electron currents; therefore a positive signal implies electron current to the electrode. Cathode and anode currents were divided by the cathode groove area to obtain the reported surface currents (A/cm<sup>2</sup>). The measured stage currents were divided by their respective active areas to obtain reported surface currents. 'Current' is used frequently to describe both quantities in this work, but the units are always given for clarity.

- The measured cathode currents were 2-3 mA/cm<sup>2</sup>, decreasing with DF. In addition, the average cathode current dropped significantly over the course of the experiments. During the pulse, there was a slow rise that did not quite reach steady state. A distinct 'ignition' spike was also observed, particularly at higher DF (see Fig 3).
- With the beam dump terminated into 50Ω, the electron current demonstrated an abrupt ignition (0.04-0.1 mA/cm<sup>2</sup>), a gradual rise to a steady state (0.3 mA/cm<sup>2</sup>) followed by a long afterglow decay. The current remained roughly the same (although cathode currents dropped significantly during experiments), but appeared to increase slightly when the large stage was present. When the beam dump was shorted directly to ground, the measured current roughly doubled and never reached a steady

state value (see Fig 3). For this reason, only current measurements with  $50\Omega$  terminations are reported.

- The small ( $50\text{ cm}^2$ ) and medium ( $600\text{ cm}^2$ ) stages showed different current measurements (see Fig 4). When positioned individually 1 cm from the e-beam edge, the small stage ion current was  $\sim 30\text{ }\mu\text{A/cm}^2$  while medium stage ion current was  $\sim 62\text{ }\mu\text{A/cm}^2$ . Overall, the ion current to the stages tracked the [varying] cathode current.
  - Figure 4 shows the current to the small stage at 10% DF; at 40% the current peaked rapidly and was fairly constant. The current to the medium stage always showed a rapid turn on phase ( $\sim 25\text{ }\mu\text{A/cm}^2$ ) followed by (1) a constantly increasing signal at 10% DF or (2) a quicker current build up and steady state value at 40% DF.
  - With both stages 1 cm from the plasma, the medium stage current was basically unchanged but the small stage signal was dramatically reduced and even changed sign.
  - When the medium stage was located over 5 cm away from the e-beam, there was still a fast ion current signal ( $\sim 2\text{ }\mu\text{A/cm}^2$ ) followed by another rapidly rising signal ( $\sim 14\text{ }\mu\text{A/cm}^2$ ) 250  $\mu\text{s}$  later (shown in Fig 3, top trace). At higher DF, more temporal variations were seen in these remote stage measurements.

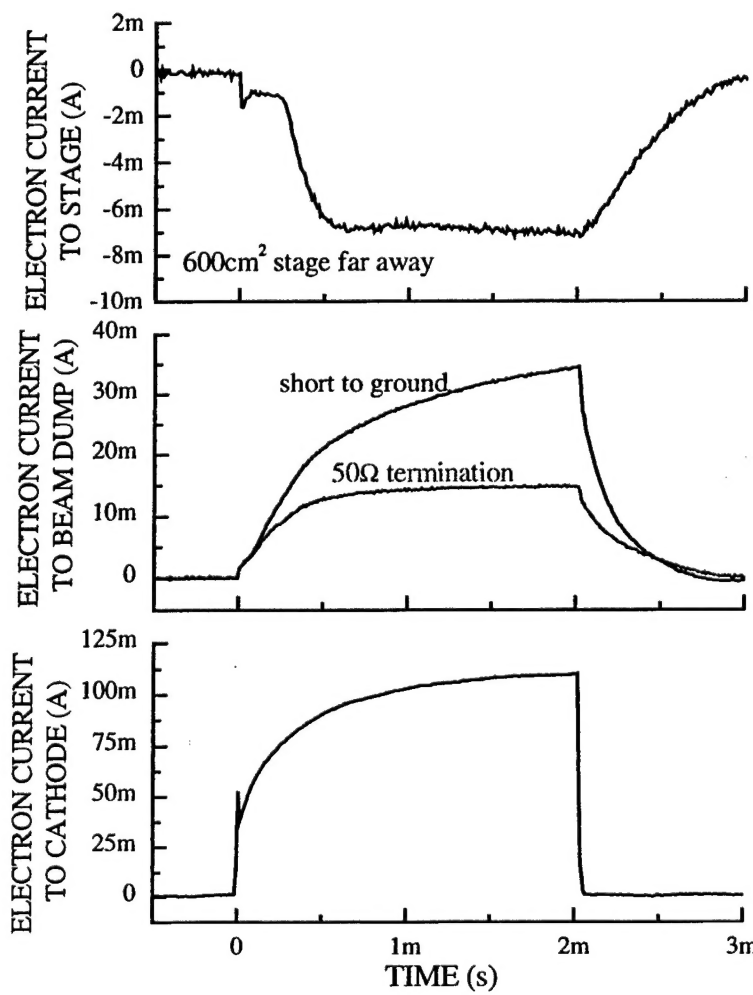


**FIGURE 3** Electron currents to cathode, beam dump and the medium stage ( $>5\text{ cm}$  from beam edge) for 10%DF plasma in large area chamber.

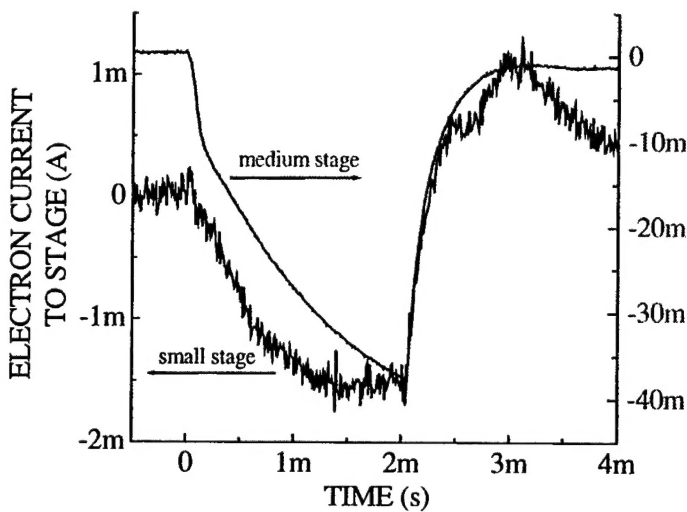


**FIGURE 4** Stage currents in the large area chamber when individually placed 1 cm from e-beam edge. Note the different axis (red) for the medium stage measurement. 10% DF.

### Discussion

*The cathode current varied throughout the entire pulse and experiment.*

- A long-term (many minutes) variance was observed in the cathode current likely due to a quasi-continuous conditioning of the cathode surfaces. It is unclear whether this conditioning was due to sputtering a specific adsorbed (or absorbed) surface layer or a phenomenon associated with ion implantation; more controlled experiments would be required to distinguish between these effects. Neither gas dynamics (i.e. heating) nor power supply operation can account for the observed decrease in cathode current with time. While the gas residence time was fairly long in this particular system (many seconds<sup>3</sup>) it is much shorter than the observed cathode current decrease. The gas therefore cannot have any thermal or electrical memory of the cathode operation on this long of a time scale. Similarly, if the power supply had been loaded down, the effects would be immediate.<sup>4</sup>
- During the pulse, the cathode current evolved continually, never quite coming to a steady state condition. The approximately exponential increase in electron current delivered to the cathode is likely due to the constantly changing load, specifically the gas dynamics inside of the hollow cathode. From the measured current density (2-3 mA/cm<sup>2</sup>) and the depth of the hollow channel (1.5 cm), an upper limit on the energy deposited into the cathode hollow volume can be calculated by  $(2 \times 10^{-3} \text{ A/cm}^2) \times (2000 \text{ V}) / (1.5 \text{ cm}) = 2.7 \text{ J/cm}^3$ . For comparison, air at 56 mtorr and 300 K has an internal energy of  $\sim 20 \mu\text{J/cm}^3$ . Thus, if even 0.001% of the calculated energy were deposited into the cathode gas volume, the temperature would double and correspondingly drop the gas density. These estimates show the possible [deleterious] effects of the cathode temperature on long pulse lengths or high duty factors.
- Although not typically discussed in processing experiments, the cathode ignition also demonstrated an interesting insight into its operation. The increase in cathode ignition current with increased duty factor implies that many charged (and/or metastable) species remain in the cathode region from the previous pulse. This

*allowed for a more pronounced ignition, separate from the gas dynamics issues mentioned previously.*

*The electron current to the beam dump anode demonstrated that this electrode was more than a beam current monitor.*

- *The variation in signal amplitude and overall temporal response implies that in addition to the beam current there was significant plasma current to the electrode. The low capacitance and resistances cannot account for such time evolutions, as the RC time constant was < 50 ns and the observed variations occur over significant fractions of a millisecond. The observed time scale was more indicative of diffusive losses of plasma current. As a brief check, the ambipolar diffusion can be estimated by<sup>5</sup>  $D_a(\text{cm}^2/\text{s}) \sim 1500[T_e(\text{eV})/\text{P}(\text{Torr})]$ , which gives  $D_a \approx 2.7 \times 10^4 \text{ cm}^2/\text{s}$  for  $T_e = 1 \text{ eV}$ . Equating this number to  $(\Delta x)^2/\tau$  and taking  $\tau \sim 1 \text{ ms}$ , the diffusion length comes out to be  $\sim 5 \text{ cm}$ , which was comparable to the distance to the closest ground (stage/chamber wall). Thus as the ions diffuse from the plasma isotropically, the electrons (near the beam dump) balance the ion current loss preferentially through the path of least resistance, along the magnetic field.*
- *The most striking evidence that the beam dump current was comprised of plasma current was the existence of the afterglow signal. In the diffusive atomic gas, the long-lived afterglow was very clear in Fig 3, where the current gradually decays from its value at the end of the cathode pulse.*
- *Upon ignition, the electron beam current should be instantaneous and roughly constant throughout the pulse. The actual electron beam current was likely the sharp rise in the signal at beginning of the pulse. (A similarly sized drop is evident at the end of the pulse.) Thus the observed waveforms consist of two components: a fast beam measurement ( $0.05\text{-}0.1 \text{ mA/cm}^2$ ) and a much larger plasma current component ( $0.2\text{-}0.3 \text{ mA/cm}^2$ ).*

*The stage currents showed fairly low ion currents, which did not scale with the size of the electrode.*

- *The larger area ( $600 \text{ cm}^2$ ) electrode typically showed twice as much ion current density than its smaller counterpart, although the temporal response for both stages follows the ion diffusion mechanism outlined previously. The fact that current to the small stage was effected by the presence of the large stage but not vice versa implied that the small stage was just a perturbation on the entire system. The small stage could be considered a planar probe in this system, although a detailed analysis of all the current paths should be more carefully considered.<sup>6</sup> The  $600 \text{ cm}^2$  stage was effectively part of a mobile chamber wall (the  $64 \text{ cm} \times 90 \text{ cm}$  stage), whereas the chamber walls behind the small stage were still major conductors of plasma current.*
- *At the higher DF, the chamber becomes flooded with ions, resulting in the observed rapid ion current response when the plasma was re-ignited. Previously the plasma diffusion time was calculated to be  $\sim 1 \text{ ms}$ ; however in the afterglow the electron temperature cools and the diffusion time can easily increase by a factor of three. Therefore, at the higher DF all of the ions cannot leave the system before the next pulse.*

- With the  $600 \text{ cm}^2$  stage further from the plasma sheet (Fig 3, top) the influence of the 'fast' and 'slow' ions can be seen. The small (fast) ion current was detected immediately upon ignition, followed by a  $500 \mu\text{s}$  delay until the bulk (slow) plasma ions can diffuse to the stage. The fast ion current could also be due to the small ion density present from the previous plasma pulse that gets accelerated to the stage upon re-ignition of the plasma. However, the fast and slow ion mechanism agrees with the mass spectrometry and langmuir probe data, which show higher electron temperatures ( $\sim 3 \text{ eV}$ ) and ion energies ( $\sim 5 \text{ eV}$ ) upon ignition and a rapid cooling after  $100-200 \mu\text{s}$ . The large size and position of the stage allow the incident ion flux to rapidly reach a steady state value.

For comparison, a nitrogen plasma (56 mT) was similarly used<sup>7</sup> to help deconvolve the effects of plasma chemistry vs cathode operation on these measurements. Figure 5 shows the complementary measurements for the  $\text{N}_2$  plasma as in Fig 3 for argon.

- The cathode current built up after an ignition phase (more pronounced for the higher DF case) and reached a steady state value of  $\sim 1 \text{ mA/cm}^2$ . The cathode current decreased throughout the experiments as in the argon case.
- The beam dump current rose very rapidly, followed by slight roll-off and steady state value of  $\sim 100 \mu\text{A/cm}^2$ . A slower build up of electron current was seen when the medium stage was present. While the cathode current dropped significantly with DF, the dump current fluctuated less than 10%. When grounded directly, the dump current was approximately twice the typical  $50\Omega$  termination value.
- The currents to the stages evolved very slowly. Ion currents were  $\sim 8 \mu\text{A/cm}^2$  to the small stage and was  $20-24 \mu\text{A/cm}^2$  to the medium stage, depending on DF.

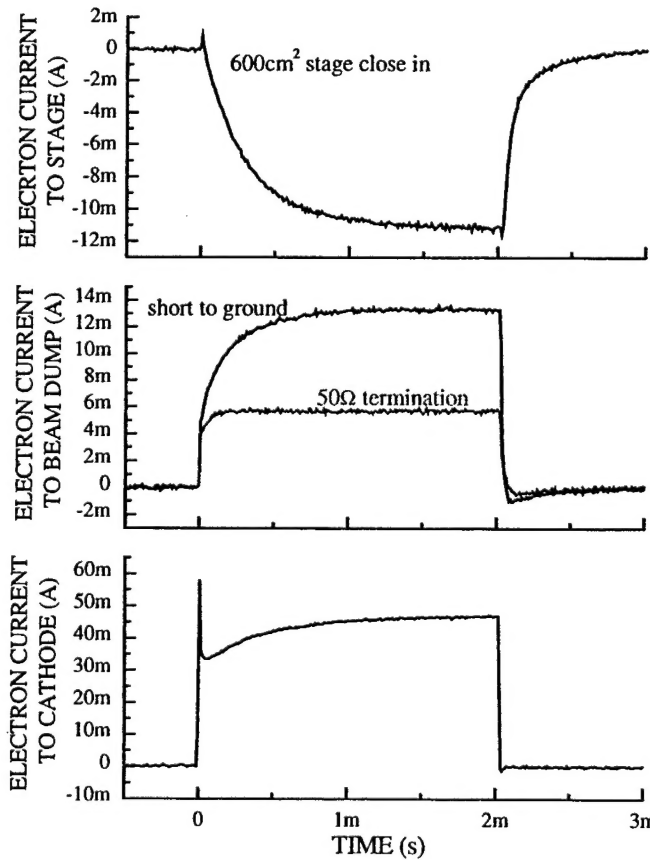


**FIGURE 5** Nitrogen plasma currents to cathode, beam dump and medium stage in large area chamber. 40% DF.

### Discussion

The cathode current measurement continued to vary over long periods of time as well as during the plasma pulse. The previously proposed mechanisms for the long term current drift (quasi-continuous conditioning of the cathode surfaces) and temporal variation during the pulse (due to gas heating) are basically independent of the actual gas, at the level of the present experiments. The cathode 'equilibration time' during the pulse was more rapid than in the argon data, which may be due to the fact that molecular gases have additional (internal) degrees of freedom that dissipate some of the energy deposited from the cathode operation. The overall lower cathode current agrees with the typical probe data that shows a smaller [beam-produced] plasma density when using these hollow cathodes in molecular vs. atomic gases. However, the variations in cathode current during the pulse were not necessarily indicative of electron beam or plasma operation, as these variations did not appear in independent probe measurements.

The beam dump currents reached steady state more rapidly than in the argon data and showed no afterglow signal. This was a marked difference from the diffusion-dominated argon plasma; recombination of  $N_2^+$  eliminated a tremendous amount of cross-field ion flow, thus the plasma electrons do not have to compensate by leaving the system along the magnetic field. The reported beam dump current should therefore be more representative of the actual beam current. However, the diffusive nature of  $N^+$  can skew these measurements, which probably accounts in part for the prolonged current build up when the beam dump was shorted to ground.

The ion current to the ( $600\text{ cm}^2$ ) stage shows a long ion current build-up, although shorter than the argon case. As mentioned previously, this current was controlled by the diffusion of ionized nitrogen species, presumably  $N^+$  flux.

As a final comparison, a mixture of argon and nitrogen (55/11 mT Ar/ $N_2$ ) was also tested.<sup>8</sup> For this mixture:

- The cathode current was  $1.4\text{ mA/cm}^2$  and the temporal responses were similar to the pure Ar case.
- The dump current was  $120\text{ }\mu\text{A/cm}^2$ . The temporal response was also similar to pure argon case, with a small fast initial current followed by a slow build up to a steady state. No afterglow signal was present.
- When both stages were inserted, the medium stage current was  $\sim 20\text{ }\mu\text{A/cm}^2$  with a very long rise time.

### Discussion

These measurements showed basically the strongest effects of each gas. The cathode and beam dump currents were in between the pure gas cases, but temporally followed the ion diffusion dominated regime. However, away from the ionization source (in the afterglow and outside the beam channel) charge exchange followed by recombination dominate, therefore no afterglow effects were seen and the currents to the stages were comparable to the pure nitrogen case.

## STAINLESS STEEL EQP CHAMBER

An argon plasma (50 mT) was run with the EQP300 mass spectrometer electrode  $\sim 2$  cm away from the beam edge.<sup>9</sup> The EQP electrode had an area of  $25 \text{ cm}^2$  and was grounded outside the chamber. The same cathode pulser unit and cabling was used in these experiments as in the previous measurements and the magnetic field was similarly solenoidal and 150 Gauss. The notable differences from the large area system are a smaller (1 cm x 25 cm x 1 cm deep) brass hollow cathode and the configuration of the anodes. Each of the anodes are made from (23 cm x 36 cm) stainless steel plates that were the inner height of the chamber (measured capacitances of  $\sim 300 \text{ pF}$ ) and terminated outside of vacuum. The slotted anode was shorted to ground in all measurements, to be consistent with the other systems. Gas flow was  $\sim 50 \text{ sccm}$ . A series of measurements at 10% DF is shown in Fig 6.

- The cathode current reached steady state faster at lower duty cycle, but showed a significant ignition spike at high DF. Steady state values were  $\sim 0.6 \text{ mA/cm}^2$ .
- The beam dump current rose sharply to a steady state value ( $0.22 \text{ mA/cm}^2$ ) and showed a long afterglow signal. When grounded directly, the current increased throughout the pulse as in the large area chamber, but was not twice the  $50\Omega$  termination value.
- The slot current showed a sharp rise to  $0.32 \text{ mA/cm}^2$  then a continual slow rise to  $1.2 \text{ mA/cm}^2$  with a long afterglow signal as well. These current values decreased with increased duty factor. (While somewhat misleading, these currents were normalized to the beam cross section, for consistency with the reported cathode and beam dump currents. In fact, the ‘active area’ of this electrode was unknown.)
- The ion current to the EQP electrode rose slowly throughout pulse at 10% DF, reaching  $140 \mu\text{A/cm}^2$ . At 40% DF, there was a rapid onset of ion current ( $90 \mu\text{A/cm}^2$ ) after a brief delay then a continual slow rise to  $160 \mu\text{A/cm}^2$ .

### Discussion

*These measurements are similar to the argon data from the large chamber, except the cathode current was much lower and reached a steady state much more rapidly. The differences between this cathode and the previous one are (1) brass vs. stainless steel construction; (2) shorter slot length; (3) shallower groove and possibly (4) different magnetic field homogeneity. Knowing that minor changes in the cathode hollow can have enormous effects on the cathode operation, the most probable reason for the decreased operation current is (3). The other nuances of the cathode operation (long and short-term temporal response) were as seen in the large area chamber data.*

*At ignition, the anode currents roughly showed a conservation of current ( $I_{\text{cathode}} \approx I_{\text{dump}} + I_{\text{slot}}$ ), but diverged drastically during the pulse. The major discrepancy was plasma electron current to the slotted anode during (and after) the pulse to compensate for the cross-field diffusion of the ions. This continual rise in the slotted anode electron current (and lack of current balance) meant that there was an unaccounted for sink of plasma ion current. The measured ion current to the EQP stage was too small to account for the excess electron current, therefore another ground larger than the EQP stage would be necessary to account for the excess [ion] current lost, probably the ground shield that surrounded the stage.*

The discontinuous ignition and decay of the anode current signals may be the electron beam current, as these rapid increases and decreases are roughly equal. If this convention is accepted, the resultant beam current was  $250\text{-}400 \mu\text{A/cm}^2$ . However, the fact that these currents are comparable at each anode implies that the slotted anode had skimmed half of the electron beam. Thus, the electron beam divergence coming out of this [shallower] cathode would have to be much larger than expected.

The ion current to the EQP electrode was larger than the previously measured ion currents in the large chamber. This result was surprising since the stage area was approximately 10% of the (single side) plasma area. Perhaps the observed increase in the ion current measurement was actually due to a decrease in electron current, which would be less likely to strike the stage two centimeters away. (The slight electron current at the beginning of the pulse is probably an artifact of the high voltage pulse.)

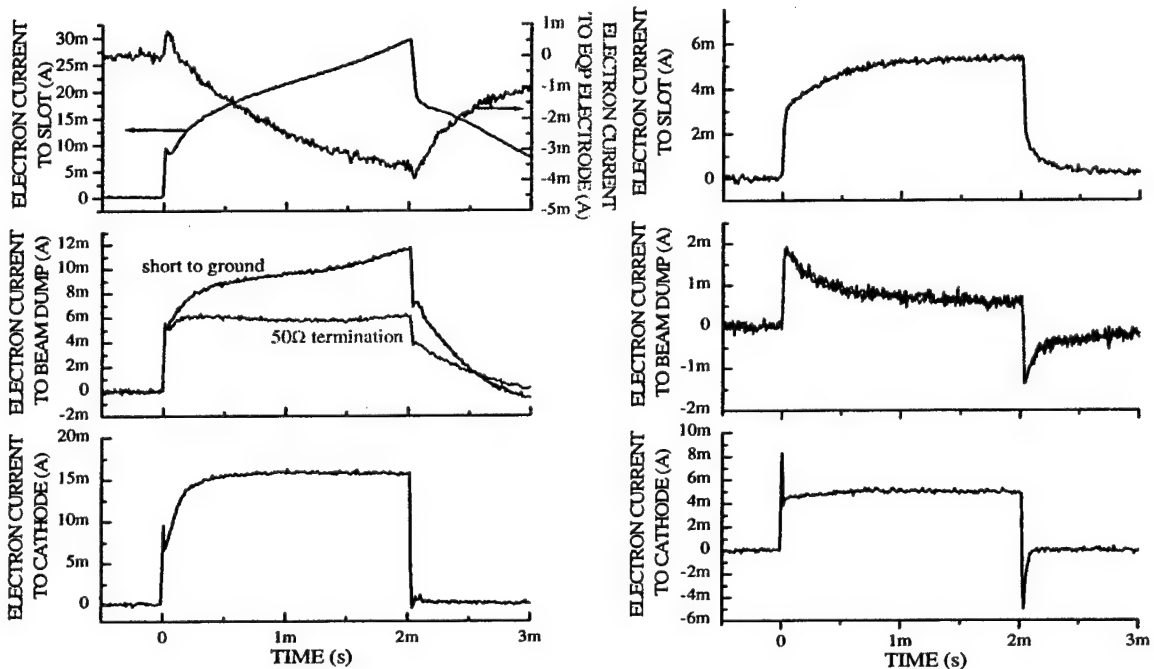


**FIGURE 6** Argon (left) and nitrogen (right) data from stainless steel EQP chamber. The current to the EQP for the nitrogen case is omitted. DF=10%.

A nitrogen plasma (55 mT) was run under the same conditions<sup>10</sup> as the previous argon plasma; a series of measurements at 10% DF is also shown in Fig 6.

- The cathode current shows dramatic turn-on/off characteristics, going immediately to a steady state ( $\sim 0.2 \text{ mA/cm}^2$ ) after an ignition spike.
- The beam dump current shows an immediate peak ( $\sim 80 \mu\text{A/cm}^2$ ) then slow decay throughout the pulse to  $22 \mu\text{A/cm}^2$ , followed by an equally rapid current change at the end of the pulse. There was no difference with dump termination.
- The slot current showed a rapid increase to  $130 \mu\text{A/cm}^2$  upon ignition then a slow rise to nearly steady state ( $200 \mu\text{A/cm}^2$ ).
- The ion current to the EQP stage was not measurable ( $< 9 \mu\text{A/cm}^2$ ).

### Discussion

Again, there was a dramatic change in the cathode operation and resultant anode currents in this system. The ideal 'top hat' cathode current can be attributed to the reduction of the gas heating effects, due to the lower applied power and the presence of a molecular gas. The very low ion current to the stage followed the trend seen in the large area system for recombination-dominated nitrogen.

The anode currents show markedly different temporal behavior; the rapid ignition of the slot electron current (3.2 mA) and the beam dump (1.8 mA) add up to the cathode current (5 mA) but the slot current increased during the pulse while the dump current disproportionately decreased. Since the electron current to the slot became larger than the cathode current, a significant amount of the slot current must be from the e-beam produced plasma. Therefore, an equal amount of ion current would have to be leaving the system. Again, the ion current to the EQP stage was too low to account for this discrepancy, thus the ground shield around the stage would be the likely current path, followed by the chamber walls. The beam dump showed a small current that rapidly decreased, implying a lesser correlation between the anodes than seen previously. Furthermore, the beam dump current was independent of the ground termination and much smaller than seen in the argon case, so either the system's plasma impedance significantly changed or a different current measurement was being made. In fact the beam dump current appeared to be a capacitive pick-up of the cathode current. This explanation supports the independent behavior of the signal with the anode termination and the observed temporal dependence. Thus the capacitive pick-up signal masked the yet smaller electron (beam and plasma) currents to the beam dump. Additional tests at various pulse lengths corroborated this possibility, but more detailed experiments focusing on the accuracy of the measurements would be necessary to determine the origin of these signals.

For a gas mixture of argon and nitrogen (50/8 mT Ar/N<sub>2</sub>) under similar operating conditions:

- The cathode current took a longer time to reach steady state ( $\sim 0.44 \text{ mA/cm}^2$ ), similar to the argon case.
- The beam dump current showed a rapid increase, peak ( $0.15 \text{ mA/cm}^2$ ) and decay of electron current ( $3 \mu\text{A/cm}^2$  at the end of the pulse). No afterglow was seen, nor does the termination show the usual 2X dependence.
- The slotted anode showed dramatic electron current onset of  $0.24 \text{ mA/cm}^2$  then a slow rise to a steady state value of  $0.54 \text{ mA/cm}^2$ .
- The EQP ion current was slowly increasing throughout the pulse, reaching  $\sim 27 \mu\text{A/cm}^2$

### Discussion

Again, these measurements showed the strongest effects of each gas, supporting the gas-phase dynamics that are frequently overlooked. The cathode operating current was closer to the pure argon case, both temporally and in magnitude whereas the slot, beam dump and stage currents were closer to the pure nitrogen case. These observations reinforce that even small amounts of molecular gases can completely change the plasma

characteristics (and therefore diagnostics) although the changes in the cathode operation remain slight.

### ALUMINUM PROCESSING CHAMBER

An argon plasma ( $50\text{ mT}$ )<sup>11</sup> was run in the aluminum processing chamber, which had three main differences when compared with the other systems: (1) A different pulser unit and power supply were used for cathode operation. (2) A pair of Helmholtz coils (25 cm radius) generated the 165 Gauss magnetic field. Most importantly (3) the cathode was an old interchangeable hollow/sleeve design, made from brass and Teflon® but the hollow part was similar in size and dimension (1 cm x 18 cm x 1.5 cm deep) as the other cathodes. A processing stage ( $100\text{ cm}^2$ ) was positioned approximately 1 cm from the beam edge. The slotted and beam dump anodes were made from 35 cm diameter plates, which were grounded outside the chamber. The slotted anode was positioned slightly inside the Helmholtz coils while the beam dump anode was slightly outside. The gas flow was  $\sim 50\text{ sccm}$ . Figure 7 shows the data described below.

- The cathode current showed a rapid current build-up and reached a steady state value of  $\sim 3.3\text{ mA/cm}^2$  without an ignition spike. A 10% drop in current was seen when the DF was increased from 10% to 40%. (A less sensitive current transformer was used for this measurement, hence the decreased S/N ratio.)
- The beam dump current increased slowly, without any obvious ignition and showed a small afterglow current. The steady state value of  $\sim 2\text{ mA/cm}^2$  was measured. When the duty factor was increased to 40%, the current rose more slowly to a steady state value  $< 1\text{ mA/cm}^2$ . Changing the termination to direct ground caused the measured current to nearly double and the afterglow signal to decay more rapidly.
- The slotted anode was grounded and showed a rapid build up of electron current with a value of  $1.5\text{ mA/cm}^2$  at 10% DF. The current switched polarity abruptly at the end

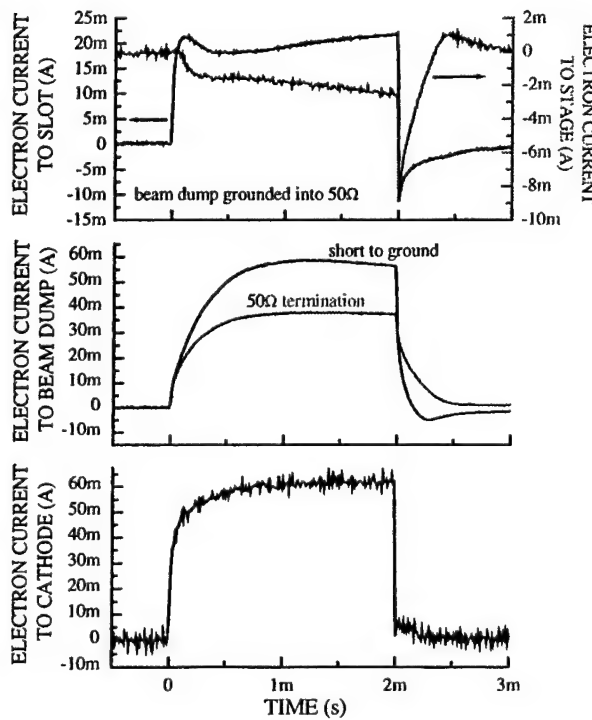


**FIGURE 7** Measured currents from argon plasma in aluminum chamber. 10% DF.

of the cathode pulse. At 40% DF, the current decreased slightly ( $1.1 \text{ mA/cm}^2$ ) during the pulse, but showed a longer-lived ion current in the afterglow. When the beam dump anode was allowed to float, the electron current to the slot rose continually throughout the plasma pulse, with an obvious afterglow signal (see Fig 8), as seen previously in the stainless steel EQP chamber.

- The ion current to the stage increased slowly to  $\sim 25 \mu\text{A/cm}^2$ . Post-pulse, there was a discontinuous increase in ion current, followed by a slow decay and eventual collection of electron current. As the beam dump termination changed, the currents to the stage changed from the ion current shown in Fig 7 to the various currents in Fig 8.

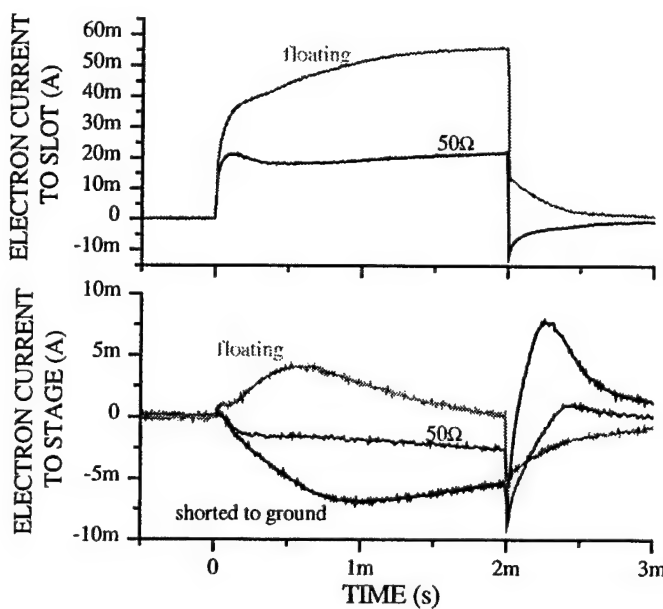


**FIGURE 8** Currents measured to the slotted anode and processing stage as the beam dump termination was varied in the aluminum chamber. Beam dump terminations are given with the corresponding plot. 10% DF.

### Discussion

The cathode current ‘equilibration’ during the pulse was similar to the other cathodes although it lacked the ignition transient. Physically, this cathode was the most massive, constructed with twice the metal (brass) as any other cathode in this study. Considering this construction, it would be reasonable that the cathode heating effects that lead to the temporal variations in cathode current would be minimized, given the high thermal conductivity (brass vs. stainless steel) and larger mass of the cathode. This was particularly advantageous since this cathode operated at the highest average current. (As discussed earlier, the current difference was likely due to the subtle differences in the hollow groove of the cathode.)

The beam dump current built up slowly, due to plasma electrons compensating for the ion cross-field diffusion. Other systems typically had an additional fast current component ( $< 5 \text{ mA}$ ), which may be masked in this data due to the large measured current. The other notable difference in this data arose post-pulse with the various terminations. When the beam dump was terminated into  $50\Omega$ , the electron current continued to follow the ion diffusion mechanism in the afterglow, but when the beam dump was shorted to ground the electron current ceased and a slight ion current was observed. (The total afterglow current was approximately zero for the data shown in Fig

8. Unfortunately, the slotted anode data had been corrupted for this case.) The origin of these afterglow current changes with the beam dump termination was unclear and cannot be explained by the primary differences in this system associated with these measurements, i.e. the spatially varying magnetic field and the over-sized anodes. These observations require additional experimental support to determine their validity and cause.

The slotted anode current was about two-thirds the current at the beam dump (also contrary to the EQP system) and showed an abrupt initiation and termination with the e-beam pulse. These rapid electron currents are most likely indicative of hollow cathode plasma current. When the cathode shut off, the current signal discontinuously switched from positive (electron) to negative (ion), which showed that there was an appreciable ion current to the slot during the high voltage pulse. However, when the beam dump was allowed to float (Fig 8), the ion current to the slot appeared to be significantly less than the electron current, as the current was positive and larger at all time. In fact, this slot current was nearly the sum of the slot and dump currents from Fig 7. Hence, when the beam dump was allowed to float (preventing a net current flow) the slotted anode became the dominant ground reference for the system's electrons. As seen previously, the plasma electrons are well confined along the magnetic field, but have to balance the diffusive ion losses and therefore travel the path of least resistance to ground (i.e. the slotted anode). However, a larger processing stage could provide an appreciable electron current path in this system, especially if the magnetic field is non-uniform.

The ion current to the stage during the beam pulse was similar to the other systems but significantly lower. As with the current to the slotted anode, the data showed a significant electron and ion flux to the stage, since only electron currents can change on the time scales seen at the end of the e-beam pulse. When the beam turned off, the large electron current ceased and ion current was measured at the stage, giving a value of  $\sim 90 \mu\text{A}/\text{cm}^2$  at the peak shown in Fig 7. In light of these observations, the current to the stage with the changing beam dump termination (Fig 8) can be better understood. As the beam dump resistance was decreased (grounded) the path of least resistance for the electron current included the beam dump, lowering the electron current to the electrodes and thus increasing the ion current signal to the stage. When the dump was left floating, the stage absorbed more of the electron current, as indicated in Fig 8. During the afterglow however, the plasma temperature and density rapidly dropped, and the stage-to-plasma separation eventually became comparable to the sheath size. Thus, the afterglow dependencies are difficult to discern with the limited information from these experiments.

As previously seen, the electron currents to the anodes decreased when the duty factor was increased from 10% to 40%. Since the largest changes occurred at the beam dump anode, the argument that the higher duty factor flooded the chamber with ions seems somewhat simplistic, since no significant compensation for the additional ion current was observed. (The currents to the stage have been ignored here, since they were always much smaller than the observed changes.)

A nitrogen plasma (55mT) was formed under similar conditions as the argon plasma.

- The cathode current showed a fast ignition spike, then similar temporal behavior as the argon case. The steady state value was  $\sim 3 \text{ mA/cm}^2$ . No significant changes with DF.
- The beam dump current also remained constant with DF, measuring  $0.3\text{-}0.4 \text{ mA/cm}^2$  when terminated into  $50\Omega$ . The current approximately doubled when the beam dump was terminated directly to ground. No changes were seen when the secondary grounded stage was inserted.
- The electron current to the slotted anode was also largely independent of DF, ranging from  $2.3\text{-}2.1 \text{ mA/cm}^2$  as DF went from 10-40%. The temporal response was different than in argon, showing a rapid turn-on and a slow build-up to steady state value (as seen in Fig 5). A slight increase in current was seen when a second grounded stage was inserted opposite the first one. The electron current to the slot increased as the electron current to the dump decreased as the dump impedance varied (see Table I).
- The stage ion current was very low ( $< 10 \mu\text{A/cm}^2$ ) and did not vary significantly with the beam dump termination (see Fig 9) during the plasma pulse. With the opposing grounded stage inserted the current was unaffected, although the signal did decrease significantly when the DF was increased.

**TABLE I** Steady-state currents to electrodes with respect to the beam dump termination.

CATHODE CURRENT (mA)	SLOT CURRENT (mA)	STAGE CURRENT (mA)	DUMP CURRENT (mA)	DUMP TERMINATION ( $\Omega$ )
55	32	< 1	17	0
55	42	< 1	6.2	50
55	50	< 1	0	$\infty$

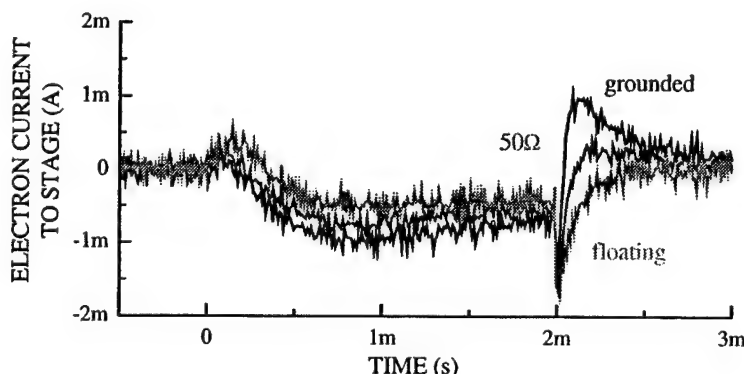


**FIGURE 9** Current to stage in  $\text{N}_2$  plasma in the aluminum chamber as beam dump termination was varied.

### Discussion

The cathode current was lower and the beam dump current equilibrated faster in nitrogen than in argon, as seen in the previous systems. Both of these effects are due to the recombinative vs. diffusive nature of the working gas discussed earlier. Also, in nitrogen the slotted anode current was significantly larger than the beam dump current,

as was also seen in the stainless steel EQP chamber for both gases (see Fig 6). This relationship between the anode currents is not surprising, since the slotted anode collects electron current from both the e-beam produced plasma and the hollow cathode discharge while the beam dump only collects electrons from the e-beam produced plasma (neglecting the much smaller e-beam current). Furthermore, when gas phase recombination localizes the plasma ions, the presence of long conduction paths of plasma electrons to balance ion losses are greatly reduced. These conditions are well illustrated by the conservation of current shown in Table I. Although there was approximately 5 mA of cathode current consistently<sup>12</sup> unaccounted for,  $I_{cath} \approx I_{dump} + I_{slot} + I_{stage}$  with the various beam dump terminations. This was the only data that preserved the current dependence and thus appears to have accounted for the dominant current paths.

The minor stage current variations with the beam dump termination seen in Fig 9 followed the trends seen in argon. However, due to the different ion transport of the molecular gas, the plasma was much 'stiffer', or resistant to changes in current flow. The minor decrease in stage ion current with increasing beam dump impedance was due to an increased electron current to the stage. After the e-beam pulse, the sharp discontinuity again implies an appreciable electron flux as seen in the argon data. In the afterglow, the ion current to the stage showed a rapid diffusive decay [of  $N^+$ ] when the beam dump was floating, which decreased with the beam dump termination. Presumably the beam dump absorbed more electron current as its resistance was decreased during the afterglow. It should also be noted that the total stage currents were only  $\sim 1\%$  of the total system current, and these small currents were not clearly discerned in the other electrode measurements.

The most striking difference in this data compared with the other systems was the lack of duty factor dependence. This observed independence could be attributed to having reduced two of the critical obstacles that result in gas heating. First, the cathode was more massive and constructed from material with high thermal conductivity (brass). Second, the molecular working gas had a high heat capacity. It should also be pointed out again that this cathode had the largest operating current of all the systems.

### STAINLESS STEEL PROCESSING ('SPUTTERING') CHAMBER

In the newly constructed stainless steel processing chamber, a similar series of plasmas<sup>13</sup> were run with a processing stage  $\sim 1$  cm away from the beam edge. The cathode was constructed from stainless steel and ceramic identical to the cathode in the large area chamber, except the channel length was 16 cm. The same cathode pulser unit and cabling was used in these measurements as in the previous EQP and Large Area Chamber measurements, although the magnetic field on this chamber was generated from a pair of Helmholtz coils. The slotted anode was mounted on the cathode support and there was no beam dump in the chamber. (The electron beam spread out well before terminating into the bottom of the chamber.) The same processing stage was used as in the aluminum processing chamber. The gas flow was  $\sim 25$  sccm.

- In all plasmas, no ion current to the processing stage (measured capacitance  $\sim 1\text{nF}$ ) was measured. Ion current could be detected only if the stage was negatively biased.

- In pure argon (55 mT), the cathode current varied from  $1.9 - 0.8 \text{ mA/cm}^2$  for 10 – 40% DF, respectively, always with a sharp ignition spike. Steady state was reached quickly ( $< 300 \mu\text{s}$ ), although it took nearly twice as long ( $\sim 600 \mu\text{s}$ ) for 10% DF case.
- In pure nitrogen (55 mT), the cathode current showed a less pronounced change with DF than the pure argon case:  $1.2 - 1.0 \text{ mA/cm}^2$  for 10 - 40% DF (respectively), but with a more pronounced ignition spike. Steady state was reached within  $300 \mu\text{s}$ , although it took slightly longer for 10% DF case.
- An argon/nitrogen mixture (55/5 mT) showed dramatic changes with DF (10-40%) as in the pure argon case:  $2.4 - 0.9 \text{ mA/cm}^2$ . Also as in the argon case, a steady state current was quickly reached, and it took approximately twice as long at 10% DF.

### Discussion

*This limited data set illustrated the previously discussed gas and cathode heating effects on the cathode operation. This system had the smallest cathode mass (with low thermal conductivity) and lowest gas flow of all the systems; thus the dramatic changes in cathode current with duty factor were not surprising. At lower duty factors the cathode could cool more between pulses, resulting in a longer time to reach steady state during each pulse. This cathode was used heavily in nitrogen plasmas and therefore probably had an extremely nitrogen-rich surface, which made it less sensitive to change in the nitrogen plasma. However, the ion bombardment of the argon plasma would change the surface composition constantly, through sputtering and changing the nitrogen-rich surface stoichiometry. Hence, on both long and short time scales it was reasonable that the argon plasma showed more dramatic changes in the cathode operation. These effects were seen in the gas mixtures as well.*

*The lack of current to the grounded stage was troublesome, until it was realized that a bias voltage was necessary. The non-measurable ion current to the ground stage meant that there was a corresponding electron current to the stage, likely due to the less-uniform magnetic field provided by the Helmholtz coils. This situation was similar to the 'grounded' beam dump case in Fig 9. However in this system, the electron beam (and plasma) was allowed to spread outside the magnetic field and terminate into various walls of the chamber. Thus, the area that terminated the beam and plasma was extremely large, well grounded and less magnetically confined. This situation should have allowed a less resistive electron path away from the stage to balance the ion diffusion across the magnetic field, thereby lowering the electron current to the stage. The fact that this was not observed implies that something else in this system allowed electron current to flow to the stage, perhaps unexpected deviations in the system's magnetic field.*

### **SUMMARY AND CONCLUSIONS**

The reported steady-state data values are summarized in Table II. Although the data sets discussed here were expected to be similar, a number of striking and important variations were seen. The origins of these differences can be generally attributed to cathode operation and/or the electron beam-produced plasma environment, and therefore used as a starting point in other systems. There was also a significant amount of data that was presented but not discussed here for various reasons, which can also serve as a starting point for future experiments.

**Table II** Summary of steady state currents measured in this work.

CHAMBER/ GAS	CURRENTS <sup>a</sup> (mA/cm <sup>2</sup> )				$\bar{B}$ <sup>b</sup>	DF dependence; Other notable observations
	$I_{cath}$	$I_{slot}$	$I_{dump}$	$I_{stage}$		
LAPPS/Ar	2-3	n/a	0.30	0.03- 0.06	s	Primarily $I_{cath}$ decreased w/increasing DF
LAPPS/N <sub>2</sub>	1.0		0.10	0.008- 0.02		Weak DF dependence Steady state reached rapidly
EQP/Ar	0.60	1.2	0.22	0.14	s	$I_{cath}$ equilibrates faster with lower DF
EQP/N <sub>2</sub>	0.20	0.20	0.022	0		Very low currents
Alum/Ar	3.3	1.5	2	0.025	h	All currents decreased with increased DF Serious current imbalance
Alum/N <sub>2</sub>	3	2.3	0.30- 0.40	0.01		Weak DF dependence Current balance
SS/Ar	1.9	n/a	n/a	n/a	h	Large drop in $I_{cath}$ w/increasing DF
SS/N <sub>2</sub>	1.2	n/a	n/a	n/a		Minor changes w/increasing DF

The cathode operation underlies many of the effects discussed in this work. The largest cathode operating currents were seen in the systems with the most massive cathodes (brass design in aluminum chamber and stainless steel design in large area chamber), although the effects of subtle differences in the actual hollow groove cannot be ruled out. Aside from these basic design considerations, gas heating and a surface 'conditioning' cause changes in long-term (many minutes) cathode operation as well as during the individual pulse. These effects are further exasperated by the working gas composition and duty factor. Molecular gases characteristically showed better long term and short term effects, due to the higher thermal conductivity (internal degrees of freedom) and gas-phase recombination. Atomic gases, which lack both of these characteristics, demonstrated severe effects on cathode operation with duty factor. To further understand these mechanisms, a more involved calculation of gas heating and transport would be essential, with complementary measurements of cathode current with respect to gas pressure. In such experiments, a careful measurement of the cathode ignition phase could also give further insight into the ion (and metastable) transport

<sup>a</sup> All currents are given with the beam dump electrode terminated into 50Ω. Cathode, slot and dump currents are normalized to the cathode slot area while stage currents are normalized to their respective active areas.

<sup>b</sup> Magnetic field geometry; s = solenoidal, h = Helmholtz.

during the operation of these cathodes and therefore the observed duty factor dependencies.

The accurate determination and interpretation of the beam dump currents was the inspiration of this body of work. From the data presented here, the beam dump current cannot be determined from a simple plate, as the plasma currents of the entire system are clearly dependent on geometry and all surrounding impedance to ground. It may be possible to consider a portion of the current collected by the beam dump as the actual e-beam current, when small sharp discontinuities are present upon ignition and termination of the e-beam pulse. Such conditions were clearly seen in the large area chamber, which also had an anode that somewhat matched the cross section of the e-beam, thereby reducing the overwhelming plasma current also typically observed in such measurements. The presence of another (i.e. slotted) anode allowed plasma currents to adjust for the varying conditions of the beam dump (terminations), since the applied magnetic field provided a preferential conduction path for the plasma electrons. Therefore, it is reasonable to assume that an actual beam current could be determined in a system with an appropriately valued termination resistor.

From the data collected and presented here, the currents measured to a processing stage placed with its surface parallel to the applied magnetic field also contained a non-trivial amount of plasma electron current. These effects appeared strongest in systems with less uniform magnetic fields (Helmholtz coils). While this observation was against the convention of magnetically confined plasma electrons, it should be pointed out that (1) the plasma electrons are only weakly confined and (2) the currents to the stage are much less than the currents to anodes aligned perpendicular to the field. The measured stage currents (per unit area) were largest for atomic gases in uniform magnetic fields, although this result is more than likely skewed due to the presence of the previously mentioned plasma electron currents. Temporally, the currents to the stage followed accepted ion diffusion mechanisms in all cases. As a function of distance, the current to a stage appeared to be dominated ion flux as the stage moved away from the plasma, with discernable velocity differences within the plasma pulse.

The other major driving force in this work was to establish the conditions where the conservation of current ( $I_{\text{cath}} \approx I_{\text{dump}} + I_{\text{slot}} + I_{\text{stage}}$ ) was upheld. It had been naturally assumed that measurements in the metal chambers would agree with measurements taken in the dielectric chambers. This work has shown that the measurement of the conservation of current is certainly possible (as seen in aluminum chamber with a nitrogen plasma), but not necessarily true (as seen in aluminum chamber with an argon plasma). The most troublesome point is that the latter data was physically inconsistent, which implied that these measurements require further experiments before a reliable conclusion can be reached.

Aside from the previously mentioned issues to be further investigated, two other areas should also be considered to complement these studies. First, the effects of the magnetic field non-uniformities were presented as the source of the discrepancy in the stage current measurements, although there were no measurements to corroborate this assumption. Second, the effects of gas mixtures were not carefully considered in terms of cathode operation or e-beam plasma behavior. This subject was somewhat neglected here because it would be large task to address in one system, let alone four. Ideally the aluminum chamber system, which had good results in the pure nitrogen case, could be

used to deconvolve both the cathode operation and plasma currents in noble gas and molecular gas mixtures.

#### **ACKNOWLEDGEMENTS**

The Office of Naval Research supported this work.

#### **REFERENCES**

<sup>1</sup> Model 110 specifications: sensitivity 0.10 V/A, 20 ns rise time, 0.8% droop/millisecond.

<sup>2</sup> See experiments on DL16-85.

<sup>3</sup> Pumping speed = Flow/Pressure = 200 sccm/60 mT =  $3.3 \times 10^3$  sccm/T =  $(3.3 \times 10^3) \times (1.27 \times 10^{-2})$  l/s  $\approx 42$  l/s.  
Residence Time = Volume/Pumping speed =  $(120 \times 120 \times 50 \text{ cm}^3) / (42 \text{ l/s}) \approx 17$  seconds.

<sup>4</sup> The charging resistor and capacitor in the power supply and pulser unit had been previously changed to allow a 10-fold increase in the deliverable power to the cathode, with no effect on these long term effects.

<sup>5</sup> M.A. Lieberman and A.J. Lichtenberg, Principles of Plasma Discharges and Materials Processing, (Wiley, New York, 1994), p. 130.

<sup>6</sup> R. Farnsler, "Ion Flux to Surfaces," NRL Code 6750 internal technical note, 15 March 1999.

<sup>7</sup> See experiments on DL16-79.

<sup>8</sup> See experiments on DL16-88.

<sup>9</sup> See experiments on DL16-89.

<sup>10</sup> See experiments on DL16-89.

<sup>11</sup> See experiments on DL16-92.

<sup>12</sup> This current was more than likely lost to the ground shield around the hollow cathode, which could not be measured.

<sup>13</sup> See experiments on DL16-91.